Explicitly Filtered Large Eddy Simulation of Two-Phase Flows with Evaporating Drops for Separating Numerical and Modelling Aspects

S. Radhakrishnan[1] and J. Bellan[1,2*]
Jet Propulsion Laboratory[1]
California Institute of Technology
Pasadena CA 91109-8099 USA
Mechanical Engineering Department[2]
California Institute of Technology
Pasadena CA 91125 USA

Abstract

To investigate whether predictions from conventional Large Eddy Simulation (LES), which are known to be grid-spacing and spatial discretization-order dependent, can be rendered grid-spacing and discretization-order independent, we have reformulated LES by explicitly filtering the non-linear terms in the governing equations [1]. The encouraging results we obtained [1] for compressible single-phase flow motivated our present study in the context of evaporating two-phase flow. Thus, we created a database through Direct Numerical Simulation (DNS) to serve, when filtered, as a template for comparisons with both conventional LES and explicitly-filtered LES (EFLES). Conventional LES is conducted with the Smagorinsky model for the gas phase, and EFLES is also performed with Smagorinsky model; the drop-field SGS model is the same in all these simulations. The results from all these simulations are compared to those from DNS and from the filtered DNS (FDNS). Similar to the single-phase flow findings, the conventional LES method yields solutions which are both grid-spacing and spatial discretization-order dependent. The EFLES solutions are found to be grid-spacing independent for sufficiently large filter-width to grid-spacing ratio, although for the highest discretization order this ratio is larger in the two-phase flow compared to the single-phase flow. For a sufficiently fine grid, the results are also discretization-order independent.

Introduction

Multiphase turbulent flows are encountered in many applications such as fuel injection and atomization in gas turbine engines. Numerical computations of multiphase turbulent flows provide a cheaper alternative to performing experiments. The most accurate method for numerically simulating the flow is based on Direct Numerical Simulation (DNS) of the governing equations in which all the scales of the flow, including the smallest dissipative scales are resolved. DNS, however, requires high computational cost and cannot be used in engineering design applications where iterations among several design conditions are necessary. Large Eddy Simulation (LES) provides a cheaper alternative to numerically simulate multiphase turbulent flows, although it has modeling requirements which do not exist in DNS. In LES only the energy-containing large scales, which are of engineering interest, are resolved and the more universal small scales are modeled thereby minimizing computational costs. The LES equations are obtained by filtering the Navier-Stokes equations. Thus, in the LES equations, the effect of the filtered small-scale motion on resolved large scale motion appears as Subgrid-Scale (SGS) terms and it represents the unresolved or "sub-grid" flow field which is unavailable; thus, these terms must be modeled. This modeling is typically done through representing the subgrid scale terms as functions of the large scale, i.e. LES, flow field. Despite great strides in LES, several unresolved problems remain. One of these problems plaguing model validation when comparing with a trusted template is the lack of grid independence. It is often assumed that the filter width is the same as the local grid spacing, an assumption which introduces considerable error in regions where the grid spacing varies drastically, as for instance in simulations where adaptive grid refinement is used in some regions to better capture the physics. An explicitly filtered (EF) LES approach is expected to mitigate some of these issues. In EFLES, the convective terms in the governing equations are explicitly filtered with a chosen filter width so that all the scales below the filter width are removed. This has the effect of removing the smallest resolved scales that are affected by numerical errors. It is hypothesized that with this explicitly filtered LES approach, the results would be independent of the spatial discretization, and this hypothesis is proved correct by the results presented below.

*Corresponding author: Josette Bellan@jpl.nasa.gov

Governing equations

The governing equations which we solve using DNS have been presented elsewhere [2] and we adopt here the same Eulerian/Lagrangian methodology. The conventional LES equations have also been presented in the past [3], and thus they will not be shown. We focus here on developing the EFLES equations.

The conventional LES formulation is devoid of a filter shape; the only effect of filtering is through the relationship between filter width and grid spacing, making the filter implicit. The truncation error may also act as an implicit filter. Clearly, this lack of knowledge regarding the filter shape poses a problem when comparing LES numerical predictions with experiments since it is uncertain how the raw experimental data should be treated for comparison with simulations. To remedy this situation, one can reformulate the LES equations by introducing an explicit filter to impose a baseline for comparing experiments and simulations. In simulations, this explicit filter has the role of suppressing higher frequencies generated due to non-linearities, thereby controlling the spectral content of the resolved flow field. Thus, in explicitly filtered LES, non-linear convective terms in the mass, momentum and energy equations, the term describing pressure work in the energy equation, as well as in the equation of the state are explicitly filtered out. Applying an explicit filter to the aforementioned non-linear terms yields

$$\frac{\partial \bar{\rho}}{\partial t} + \frac{\partial \left(\overline{\bar{\rho}\tilde{u}_j}\right)}{\partial x_j} = \bar{S}_I, \tag{1}$$

$$\frac{\partial \left(\bar{\rho}\tilde{u}_i\right)}{\partial t} + \frac{\partial \overline{\left(\bar{\rho}\tilde{u}_i\tilde{u}_j\right)}}{\partial x_j} = -\frac{\partial \left[p\left(\bar{\phi}\right)\right]}{\partial x_i} + \frac{\partial \sigma_{ij}\left(\bar{\phi}\right)}{\partial x_j} + \bar{S}_{II,i} - \frac{\partial \tau_{ij}^{ef}}{\partial x_j}, \tag{2}$$

$$\begin{aligned}\frac{\partial \left(\bar{\rho}\tilde{e}_t\right)}{\partial t} + \frac{\partial \overline{\left(\bar{\rho}\tilde{e}_t\tilde{u}_j\right)}}{\partial x_j} = &-\frac{\partial \overline{\left[p\left(\bar{\phi}\right)\tilde{u}_j\right]}}{\partial x_j} - \frac{\partial q_j\left(\bar{\phi}\right)}{\partial x_j} + \frac{\partial \left[\sigma_{ij}\left(\bar{\phi}\right)\tilde{u}_i\right]}{\partial x_j} + \bar{S}_{III} \\ &- \frac{\partial \zeta_j^{ef}}{\partial x_j} - \frac{\partial}{\partial x_j}\left(\tau_{ij}^{ef}\tilde{u}_i\right),\end{aligned} \tag{3}$$

$$\frac{\partial(\bar{\rho}\tilde{Y}_V)}{\partial t} + \frac{\partial \overline{\left(\bar{\rho}\tilde{Y}_V\tilde{u}_j\right)}}{\partial x_j} = -\frac{\partial j_{Vj}\left(\bar{\phi}\right)}{\partial x_j} + \bar{S}_I - \frac{\partial \eta_j^{ef}}{\partial x_j} \tag{4}$$

where S_I, $S_{II,i}$ and S_{III} are source terms due to interaction of the drops with the gas. The thermodynamic variables to be computed from ϕ are the internal energy ($e = e_t - e_k$, where the kinetic energy is $e_k = u_i u_i/2$), the pressure (p), the temperature (T) and the enthalpy ($h = e + p/\rho$).

Quantities τ_{ij}^{ef}, ζ_j^{ef} and η_j^{ef} in Eqs. (2)–(4) are the SGS terms for explicitly filtered case (denoted by superscript *ef*) and are different from the SGS terms that appear in the conventional LES equations

$$\tau_{ij}^{ef} = \overline{\rho u_i u_j} - \overline{\bar{\rho}\tilde{u}_i\tilde{u}_j}, \quad \zeta_j^{ef} = \overline{\rho h u_j} - \overline{\bar{\rho}\tilde{h}\tilde{u}_j}, \quad \eta_j^{ef} = \overline{\rho Y_V u_j} - \overline{\bar{\rho}\tilde{Y}_V\tilde{u}_j}, \tag{5}$$

We assume that the perfect gas equation of state

$$p\left(\phi\right) = \rho R\left(\phi\right) T\left(\phi\right), \tag{6}$$

holds where $R\left(\phi\right) = Y_V R_V + Y_C R_C$, $R_V = R_u/m_V$, $R_C = R_u/m_C$, R_u is the universal gas constant and m_C and m_V are the molar weights of the carrier gas and vapor respectively, and

$$h\left(\phi\right) = h_V Y_V + h_C Y_C, \tag{7}$$

where h_C and h_V are the enthalpies of the pure gases,

$$h_C = \int C_{p,C}\left(T\right) dT, \qquad h_V = \int C_{p,V}\left(T\right) dT, \tag{8}$$

calculated from a specified functional form of the heat capacities at constant pressure, $C_{p,C}$ and $C_{p,V}$. Since the equation of the state is non-linear, it is filtered to obtain the pressure as

$$\bar{p}\left(\phi\right) = \overline{\bar{\rho}\tilde{R}\left(\bar{\phi}\right)\tilde{T}\left(\bar{\phi}\right)}, \tag{9}$$

The Filtered Source Terms (FSTs) ($\bar{S} = \left\{\bar{S}_I, \bar{S}_{II,i}, \bar{S}_{III}, \bar{S}_I\right\}$) are properly interpreted by considering a drop located at $\vec{X}$ within the filtering volume V_f and its contribution within that volume

$$\bar{S}\left(\vec{x}\right) = \int_{V_f} S_d \delta(\vec{y} - \vec{X}) G\left(\vec{x} - \vec{y}\right) d\vec{y}, \tag{10}$$

where $S_d\delta(\vec{y} - \vec{X})$ is the point-source contribution from the drop and δ is the delta function. When G is a top-hat filter, the FST is

$$\bar{S}\left(\psi_f, Z\right) = \frac{1}{V_f} \sum_{\beta} \left[S_d\left(\psi_f, Z\right)\right]_\beta, \tag{11}$$

a volume-average over the drops β within the filtering volume. Since $\bar{S}$ is not known in LES, it must be modeled by invoking $\overline{\phi}$. Similarly, if the drop field to which the β drop belongs is different from that to which the α drop belongs, there will also be a drop-field model. Because the drop-field model is at a scale smaller than the LES grid, this is called a drop-field SGS model. This terminology is consistent with the $\bar{S}\left(\psi_f, Z\right)$ functional dependence upon both gas-field and drop-field variables. Equations (10) and (11) are the same in LES and EFLES except that the vector ψ_f is based for EFLES on the solution of the explicitly filtered LES equations.

SGS models: gas and drops

To delineate the difference between LES and EFLES SGS models, both of them are presented below.

Conventional LES model: The Smagorinsky [4, 5] model is an eddy viscosity model derived assuming that the production of the subgrid scale turbulent kinetic energy is in balance with the dissipation of the subgrid scale turbulent kinetic energy. In this model

$$\tau_{ij} - \frac{1}{3}\tau_{kk}\delta_{ij} = -2C_{SM}^2 \bar{\Delta}^2 \overline{\rho} \left|S\left(\bar{\phi}\right)\right| \left[S_{ij}\left(\bar{\phi}\right) - \frac{\delta_{ij}}{3} S_{kk}\left(\bar{\phi}\right)\right], \tag{12}$$

where $S^2\left(\phi\right) = 2S_{ij}\left(\phi\right) S_{ij}\left(\phi\right)$ and the Yoshizawa [6] (YO) model is used to compute

$$\tau_{kk} = C_{YO} \bar{\Delta}^2 S^2\left(\bar{\phi}\right). \tag{13}$$

The SGS scalar fluxes, vapor mass fraction or enthalpy, are modeled as

$$\eta_j = -C_{SM}^2 \frac{\bar{\Delta}^2 \overline{\rho} \left|S\left(\bar{\phi}\right)\right|}{Pr_{sgs}} \frac{\partial \widetilde{Y}_v}{\partial x_j}, \tag{14}$$

$$\zeta_j = -C_{SM}^2 \frac{\bar{\Delta}^2 \overline{\rho} \left|S\left(\bar{\phi}\right)\right|}{Sc_{sgs}} \frac{\partial \widetilde{h}}{\partial x_j}. \tag{15}$$

Coefficients C_{SM}, and Pr_{sgs}, which is interpreted as a SGS Prandtl number, are computed through the dynamic coefficient computation described in Martin et al. [7] and the model name is abbreviated as LES-DSM.

EFLES model: The Smagorinsky model for the SGS stresses is reformulated by applying an explicit filter to Eq. (12) so as to remove the scales below the filter width that are generated by the non-linearity of the model

$$\tau_{ij}^{ef} - \frac{1}{3}\tau_{kk}^{ef}\delta_{ij} = \overline{-2C_{SM} \bar{\Delta}^2 \overline{\rho} \left|S\left(\bar{\phi}\right)\right| \left[S_{ij}\left(\bar{\phi}\right) - \frac{\delta_{ij}}{3} S_{kk}\left(\bar{\phi}\right)\right]}, \tag{16}$$

The Yoshizawa model for the trace term is

$$\tau_{kk}^{ef} = \overline{C_{YO} \bar{\Delta}^2 S^2\left(\bar{\phi}\right)}. \tag{17}$$

The SGS scalar fluxes, vapor mass fraction or enthalpy, are modeled as

$$\eta_j^{ef} = \overline{-C_{SM}^2 \frac{\bar{\Delta}^2 \overline{\rho} \left|S\left(\bar{\phi}\right)\right|}{Pr_{sgs}} \frac{\partial \widetilde{Y}_v}{\partial x_j}}, \tag{18}$$

$$\zeta_j^{ef} = \overline{-C_{SM}^2 \frac{\bar{\Delta}^2 \overline{\rho} \left|S\left(\bar{\phi}\right)\right|}{Sc_{sgs}} \frac{\partial \widetilde{h}}{\partial x_j}}. \tag{19}$$

Coefficients C_{SM}, and Pr_{sgs}, which is interpreted as a SGS Prandtl number, are computed through the dynamic coefficient computation described in Martin et al. [7] and the model name is abbreviated as EFLES-DSM.

Filtered source terms model: In LES, the effect of the drops on the gas phase occurs through the filtered source terms (FSTs), $\bar{S}$. To compute $\bar{S}$ through Eq. (11), one must have models for both the unfiltered variables at the drop far-field (ψ_f) and the drop state (Z). Because ψ_f is not available in LES, it must be modeled from the simulated flow field ($\bar{\phi}$), leading to $\psi_{f,m}$. We follow here the strategy of Leboissetier *et al.* [3] in using the filtered flow field at the drop location as a model for the unfiltered flow field (i.e. $\psi_{f,m} = \tilde{\psi}_f$), which means that we neglect direct SGS flow effects on the drops' evolution.

Regarding Z, we follow the LES spirit of reducing the resolution requirements and as in [2] we simulate a reduced drop field, here denoted $\bar{Z}$, implying that $\bar{S}$ now must be modeled from $\bar{Z}$. The model of Z through $\bar{Z}$ represents the drop-field SGS model. Defining the filtered gas-phase primitive variables as $\tilde{\psi} = \{\tilde{u}_i, \tilde{T}, \tilde{Y}_V, \bar{p}\}$, then consistent with the gas-phase equations, $\tilde{\psi}(\bar{\phi})$ takes the same form as $\psi(\phi)$.

Following [2] and considering that experimental measurements only provide the total number of drops, we make a 'blind' choice to represent the physical drops (Z) by a computational drop field ($\bar{Z}$) in which each computational drop represents a number, N_R, of physical drops:

$$N_R = N_\alpha / N_\beta \tag{20}$$

is the ratio between the number of physical drops, N_α, and the number of computational drops, N_β. The FSTs are then computed for the N_β drops, and scaled by N_R leading to

$$\bar{S}_m\left(\psi_{f,m}\left(\bar{\phi}\right), \bar{Z}\right) = N_R \sum_\beta \frac{1}{V_f}\left[S_d\left(\psi_{f,m}\left(\bar{\phi}\right), \bar{Z}\left(N_R\right)\right)\right]_\beta . \tag{21}$$

As in Eq. (11), the summation is over the drops within the filtering volume V_f, but now over a representative drop field ($\bar{Z}$) rather than the physical drops (Z). The source term contributions for each computational drop are calculated in the same manner as for physical drops, that is, the representative nature of each drop is entirely manifested in the parameter N_R. Thus, changing the value of N_R is tantamount to changing the FST (i.e. the drop-field SGS) model.

Numerical methods

Direct Numerical Simulations were performed using a fourth-order explicit Runge-Kutta scheme for temporal integration, an eighth-order central finite differencing scheme for spatial discretization and a sixteenth-order filter to remove aliasing errors [8]. The non-linear terms in the governing equation were recast in cubic skew symmetric form, as proposed by Kennedy and Gruber [9], to reduce aliasing error. A fourth-order Lagrange interpolation procedure is used to obtain gas-phase variable values at the drop locations [10]. The same numerical scheme is used in LES except for the second derivative viscous terms. For these second derivative terms in the LES governing equations, eighth order narrow stencils proposed by Mattsson and Nordstrom [11] were used. The narrow stencil discretization provides better diffusion for the highest resolved wavenumbers and it was found unnecessary to apply de-aliasing filter in LES calculations. Details of the filter applied in EFLES calculations can be obtained from Radhakrishnan and Bellan[1].

Problem formulation

The physical configuration is that of a temporal mixing layer having streamwise (x_1), the cross-stream (x_2), and the spanwise (x_3) dimension of 0.6m, 0.45m and 0.15m respectively. Periodic boundary conditions are used in the x_1 and x_3 directions, and an adiabatic slip wall condition is used at the x_2 boundaries [12]. In LES simulations, this treatment led to instabilities at the x_2 boundaries and a sponge layer near the x_2 boundaries was needed to keep the simulation stable. Drops reaching the slip walls are assumed to stick to the wall, but are otherwise transported according to the drop equations. Initially, the gas phase consists only of the carrier gas (air with no vapor); the initial mean streamwise velocity has an error-function profile. To promote transition to turbulence, the layer is initially perturbed with homogeneous turbulence. We add broadband fluctuations, similar to the one used by Pantano and Sarkar [13]. The turbulence intensity is 10%, it is added only in the shear-layer and gradually decays to zero as one moves away from the shear layer along the cross-stream direction. This description pertains to the DNS. For LES or EFLES, the initial conditions are those of the filtered DNS (FDNS) at $t^{**} \equiv t\Delta U_0/\delta_{\omega,0} = 100$ when the flow transitioned to turbulence.

Initially, 71,411,456 n-decane drops, corresponding to a mass loading (ratio of liquid mass to the carrier gas mass) of 0.2, are randomly distributed throughout the bottom half ($x_2 < 0$) of the domain. The initial velocity of each drop is the same as that of the gas phase at its location. The drops interact only dynamically with the flow up to $t^{**} = 100$,

after which the drops are allowed to evaporate and the computation is conducted up to $t^{**} = 250$. At $t^{**} = 100$, the drops are at a temperature of 345 K which is lower than the boiling point (447.7 K) of n-decane, and also lower than the temperature of air (375 K). The drop size variation is specified by a Gaussian distribution such that the initial Stokes number ($St \equiv \tau_d \Delta U_0/\delta_{\omega,0}$) mean is 3 and the standard deviation is 0.5.

Results

The DNS database consists of a single simulation initiated with $\mathrm{Re}_0 = 1200$, $M_{c,0}$=0.35, $T_{C,0}$=375K, ρ_0=0.9415kg/m^3, ΔU_0=271.7m/s and $\delta_{\omega,0}$=6.667$\times 10^{-3}$m. The number of grid nodes along the streamwise, the cross-stream and the spanwise directions ($N_1 \times N_2 \times N_3$) is 1120 $\times$ 840 $\times$ 280, and the ratio of the grid spacing to the Kolmogorov scale is $\Delta_{DNS}/\eta_K = 2.5$. At $t^{**} = 0$, $\delta_{m,0}/\delta_{\omega,0}$ =0.22475, where

$$\delta_m = \frac{1}{\rho_0 \Delta U_0^2} \int_{-L_2}^{L_2} \rho \left(0.5\Delta U_0 - \frac{\langle \overline{\rho}\widetilde{u}_1 \rangle}{\langle \overline{\rho} \rangle}\right) \left(0.5\Delta U_0 + \frac{\langle \overline{\rho}\widetilde{u}_1 \rangle}{\langle \overline{\rho} \rangle}\right) dx_2 \tag{22}$$

measures the growth of the mixing layer. The layer achieves self-similarity at $t^{**} = 60$ when the growth of δ_m becomes linear. As already stated, the simulation is conducted up to $t^{**} = 250$ at which time station $\delta_m/\delta_{\omega,0}$ =3.2629 and $\mathrm{Re}_m \equiv \rho_0 \Delta U_0 \delta_m/\mu = 3915.2$.

Both LES and EFLES were performed with coarse (C), medium (M) or fine (F) grids and for various discretization orders: fourth (grids C4, M4 or F4), sixth (grids C6, M6 or F6) or eight (grids C8, M8 or F8) order. The number of nodes were 280 $\times$ 210 $\times$ 70, 560 $\times$ 420 $\times$ 140 and 1120 $\times$ 840 $\times$ 280 in the C, M and F grids, respectively. In LES, $\bar{\Delta} = \Delta_{LES}$ and is respectively $4\Delta_{DNS}$ and $2\Delta_{DNS}$ for the C and M grids. In EFLES, $\bar{\Delta}$ =$8\Delta_{DNS}$ independent of grid spacing which is $4\Delta_{DNS}$, $2\Delta_{DNS}$ and Δ_{DNS} for the C, M and F grids, respectively.

As shown in Fig. 1, in the central part of the layer there is a wide discrepancy among Reynolds stress predictions according to grid spacing and spatial discretization order. For $\langle \rho u_1'' u_1'' \rangle / \rho_0 \Delta U_0^2$ ($\psi'' = \psi - < \psi >_{LES}^F$ where $< \psi >_{LES}^F = < \overline{\rho\psi} > / < \overline{\rho} >$), in contrast to the single-phase flow results, all LES predictions underestimate rather than overestimate the DNS as well as the two FDNS obtained with different filter widths. However, both $\langle \rho u_2'' u_2'' \rangle / \rho_0 \Delta U_0^2$ and $\langle \rho u_3'' u_3'' \rangle / \rho_0 \Delta U_0^2$ still tend to overestimate and better approximate the DNS rather than the FDNS. For $\langle \rho u_1'' u_2'' \rangle / \rho_0 \Delta U_0^2$, the FDNS very closely follows the DNS , and thus which template is better reproduced is not an issue, however, unlike in single-phase flow, the LES do not consistently overestimate the template over the ξ range. Apparently, the presence of drops modifies the total dissipation so that conclusions obtained for single-phase flows are not necessarily valid for two-phase flow.

The Reynolds stresses obtained from the EFLES employing the dynamic Smagorinsky model and $N_R = 8$ are depicted in Fig. 2. Compared with the situation for conventional LES (Fig. 1), here the predictions of all simulations are bunched in a considerably narrower band. For all Reynolds stresses, EFLES-DSM-M6-1200 and EFLES-DSM-M8-1200 simulations produce coinciding results, with EFLES-DSM-M4-1200 showing only small deviation from the other two medium-grid simulations. However, none of the coarse-grid predictions exhibit close agreement among them or with the medium-grid results. Moreover, all EFLES calculations overestimate the magnitude of the FDNS stresses (and also those from DNS), with a single exception for $\langle \rho u_1'' u_1'' \rangle / \rho_0 \Delta U_0^2$ at and in the vicinity of $\xi = 0$.

We also considered here a fine grid motivated by the fact that unlike in the single-phase EFLES study [1] where the results for coarse and medium grids matched for the eighth-order scheme, the results from the coarse grid do not match for two-phase flow with those of the medium grid even for the eighth-order scheme. Thus, to obtain an increased perspective, similar to the single-phase flow study, it was deemed necessary to also perform EFLES calculations on a fine grid to inquire whether grid-spacing independence can be obtained by further mesh refinement. Figure 3 illustrates these results and shows that the fine-grid calculations match for all orders of discretization and additionally they coincide with the results from EFLES-DSM-M6-1200 and EFLES-DSM-M8-1200 calculations, with the EFLES-DSM-M4-1200 predictions only negligibly dissenting. This implies that for the fourth to eighth discretization orders, the medium grid is sufficiently refined to represent grid-spacing-independent results since further grid refinement yields the same solution, and additionally, the medium grid is also sufficient to obtain discretization-order independence from the fourth to eighth orders. Further refinement to the fine mesh seems thus unnecessary.

Additional to the Reynolds stresses, comparisons were also made at $t^{**} = 250$ for the drop distribution with respect to regions of given vorticity rate and strain rate, and for the probability distribution function of the Stokes number (figures not shown due to space constraints). The results entirely support the findings for the Reynolds stresses. Also consistent with the Reynolds-stress findings were second-order correlations for the vapor mass fraction fluctuations, $\langle \rho Y_v'' Y_v'' \rangle / \rho_0$, and their flux, $\langle \rho u_2'' Y_v'' \rangle / \rho_0 \Delta U_0$ (figures not shown due to space constraints). The ensemble of these quantities indicated that explicit filtering of the conservation equations can indeed separate modelling and numerical

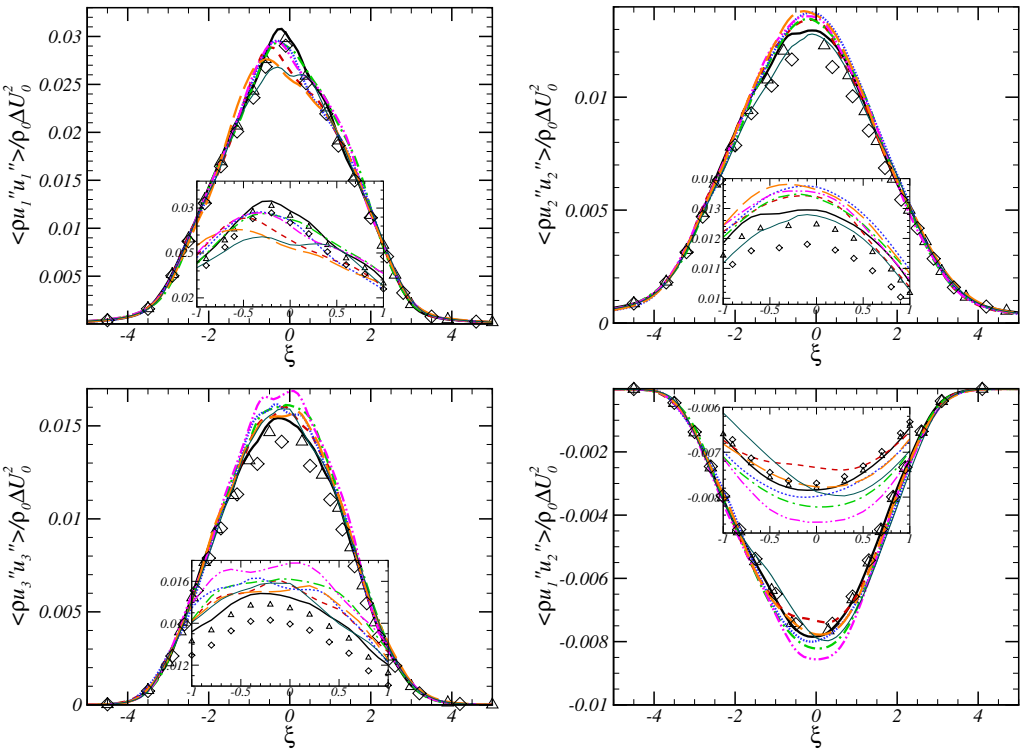

Figure 1. Reynolds stress prediction. ——— DNS; △ filtered DNS with $\bar{\Delta} = 2\Delta_{DNS}$; ◇ filtered DNS with $\bar{\Delta} = 4\Delta_{DNS}$; - - - LES-DSM-M8-1200; -·- LES-DSM-C8-1200; ····· LES-DSM-M6-1200; -·-·- LES-DSM-C6-1200; ——— LES-DSM-M4-1200; ——— LES-DSM-C4-1200.

aspects, additional to providing a filter shape and scale (i.e. the filter width) which can be used both in experiments and simulations to obtain a meaningful model evaluation with data.

Summary and Conclusions

The explicitly filtered Large Eddy Simulation (EFLES) formulation which has been previously developed and examined for compressible single-phase flows, has been here formulated and assessed for two-phase flows with phase change. Similar to the single-phase EFLES formulation, the small-scale producing nonlinear terms in the governing equations are explicitly filtered, and this procedure is applied both to the differential equations and to the equation of state. We examined whether the single-phase results can be replicated in the two-phase case. First, we created a template database of Direct Numerical Simulation (DNS) which portrays the evolution of an initially-perturbed three-dimensional shear layer laden with evaporating droplets; this template has served as the basis for comparison determining the accuracy of both conventional LES and EFLES.

Both conventional LES and EFLES computations have been conducted with Subgrid-Scale (SGS) models which are of two generic types: for the gas phase and for the drop-field. For conventional LES, the filter width was chosen to be equal to the grid spacing. For EFLES, the filter width was independent of the grid spacing. Results were obtained at three different spatial discretization orders - fourth order, sixth order and eighth order - and with either a coarse or a medium grid for conventional LES, and with a coarse, medium or a fine grid for EFLES. Examination of these results revealed that unlike for conventional LES where the results are always grid dependent, the EFLES results are grid-independent for sufficiently large filter-width to grid-spacing ratio. The EFLES results were independent of the drop-field SGS models used for the range examined here.

Acknowledgments

This study was conducted at the Jet Propulsion Laboratory (JPL), California Institute of Technology (Caltech) and sponsored by NASA jointly under the Fundamental Aeronautics Program with Drs. Dan Bulzan and Nan-Suey Liu

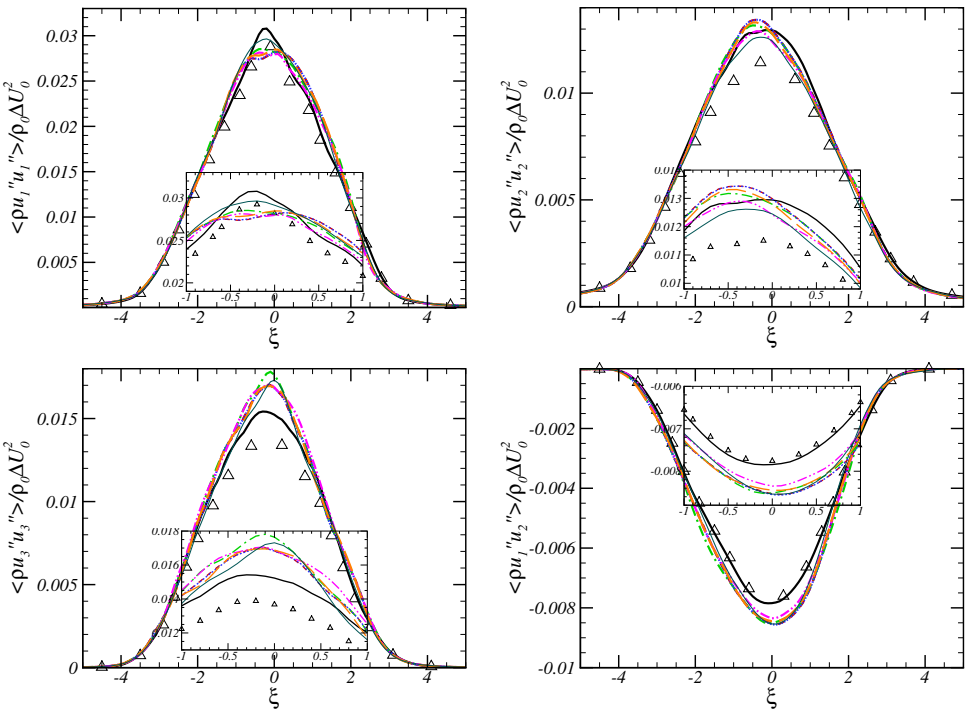

Figure 2. Reynolds stress prediction from EFLES using the dynamic Smagorinsky model and $N_R = 8$. ——— DNS; △ filtered DNS; - - - EFLES-DSM-M8-1200; -·-·- EFLES-DSM-C8-1200; ····· EFLES-DSM-M6-1200; -··-·- EFLES-DSM-C6-1200; ——— EFLES-DSM-M4-1200; ——— EFLES-DSM-C4-1200.

serving as program monitors, and under the LASER program in the ESMD/Advanced Capabilities Division.

References

1. Radhakrishnan, S. and Bellan, J., *J. Fluid Mech.* in press (2012).
2. Okong'o, N. and Bellan, J., *J. Fluid Mech.* 499:1-47 (2004).
3. Leboissetier, A., Okong'o, N. and Bellan, J., *J. Fluid Mech.* 523:37-78 (2005).
4. Smagorinsky, J., *Mon. Weather Rev.* 91:99–164 (1963).
5. Smagorinsky, J., *Large Eddy Simulation of Complex Engineering and Geophysical Flows*, edited by B. Galperin and S. Orszag, chap. 1, Cambridge University Press, 3–36 (1993).
6. Yoshizawa, A., *Phys. Fluids* 29(7):2152–2164 (1986).
7. Martin, M. P., Piomelli, U. and Candler, G. V., *Theor. and Comp. Fluid Dyn*. 13:361-376 (2000).
8. Kennedy, C. and Carpenter, M., *Appl. Num. Math.* 14:397–433 (1994).
9. Kennedy, C. A. and Gruber, A., *J. of Comp Phys*. 227(3):1676-1700 (2008).
10. Miller, R. S. and Bellan, J., *J. Fluid Mech.* 384:293-338 (1999).
11. Mattsson, K. and Nordstrom, J., *J. Comput. Phys.* 199:503–540 (2004).
12. Poinsot, T.J. and Lele, S.K., *J. Comp. Phys.* 101:104-129 (1992).
13. Pantano, C. and Sarkar, S., *J. Fluid Mech.* 451 329-371 (2002).

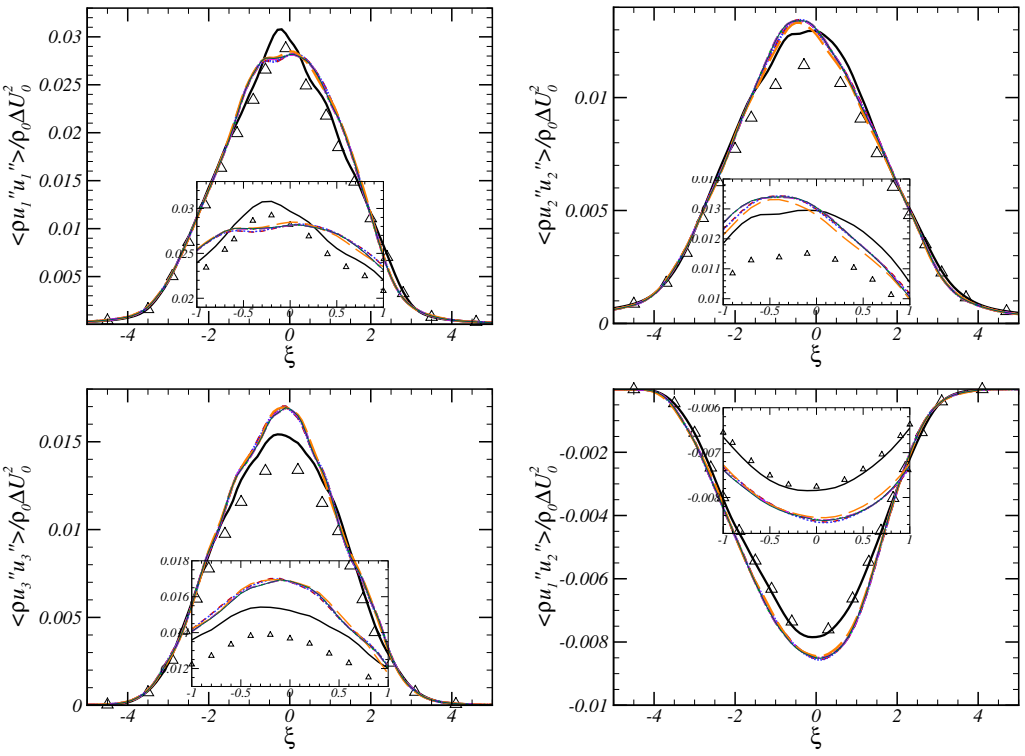

Figure 3. Reynolds stress prediction from EFLES using the dynamic Smagorinsky model. ——— DNS; △ filtered DNS; – – – EFLES-DSM-M8-1200; –·– EFLES-DSM-F8-1200; ····· EFLES-DSM-M6-1200; –··– EFLES-DSM-F6-1200; ——— EFLES-DSM-M4-1200; ——— EFLES-DSM-F4-1200.